Supporting Information

Wan and Stubbs 10.1073/pnas.1322933111

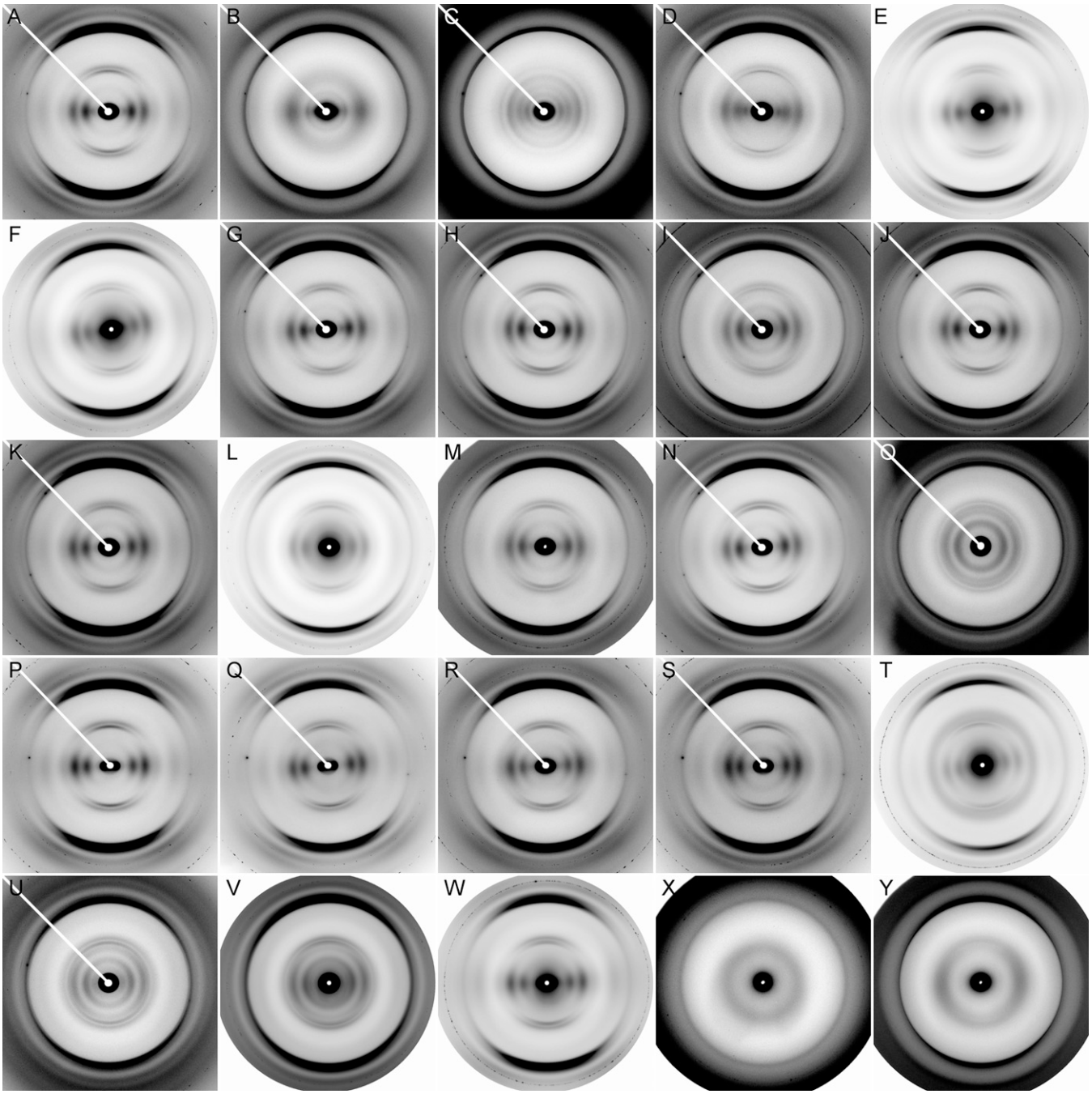

Fig. S1. X-ray fiber diffraction from HET-s(218–289) mutants. (*A*) WT, (*B*) RL, (*C*) SL, (*D*) Δ251–253, (*E*) PA, (*F*) PB, (*G*) PAB, (*H*) SA−, (*I*) SB−, (*J*) SC−, (*K*) SABC−, (*L*) SB+, (*M*) SA+, (*N*) SC+, (*O*) SABC+, (*P*) NA, (*Q*) NB, (*R*) NC, (*S*) ND, (*T*) NAB, (*U*) NAD, (*V*) NBC, (*W*) NCD, (*X*) SN−, and (*Y*) SN+.

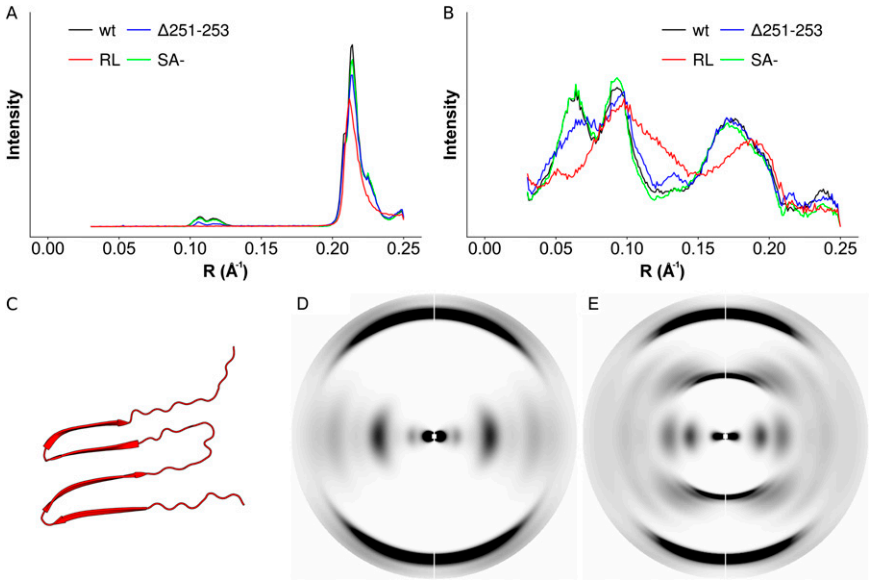

Fig. S2. Representative plots and simulated X-ray diffraction. (*A*) Meridional and (*B*) equatorial plots from WT, Δ251–253, RL, and SA−. SA− has diffraction nearly identical to that of WT, whereas Δ251–253 has a similar equator and an attenuated 9.4-Å meridional reflection. RL has a substantially different equator and no 9.4-Å meridional reflection. (*C*) A generic stacked β-sheet model and (*D*) its calculated diffraction pattern. (*E*) Calculated diffraction pattern from the two-rung β-solenoid solid-state NMR structure of HET-s(218–289) (PDB ID code 2kj3).

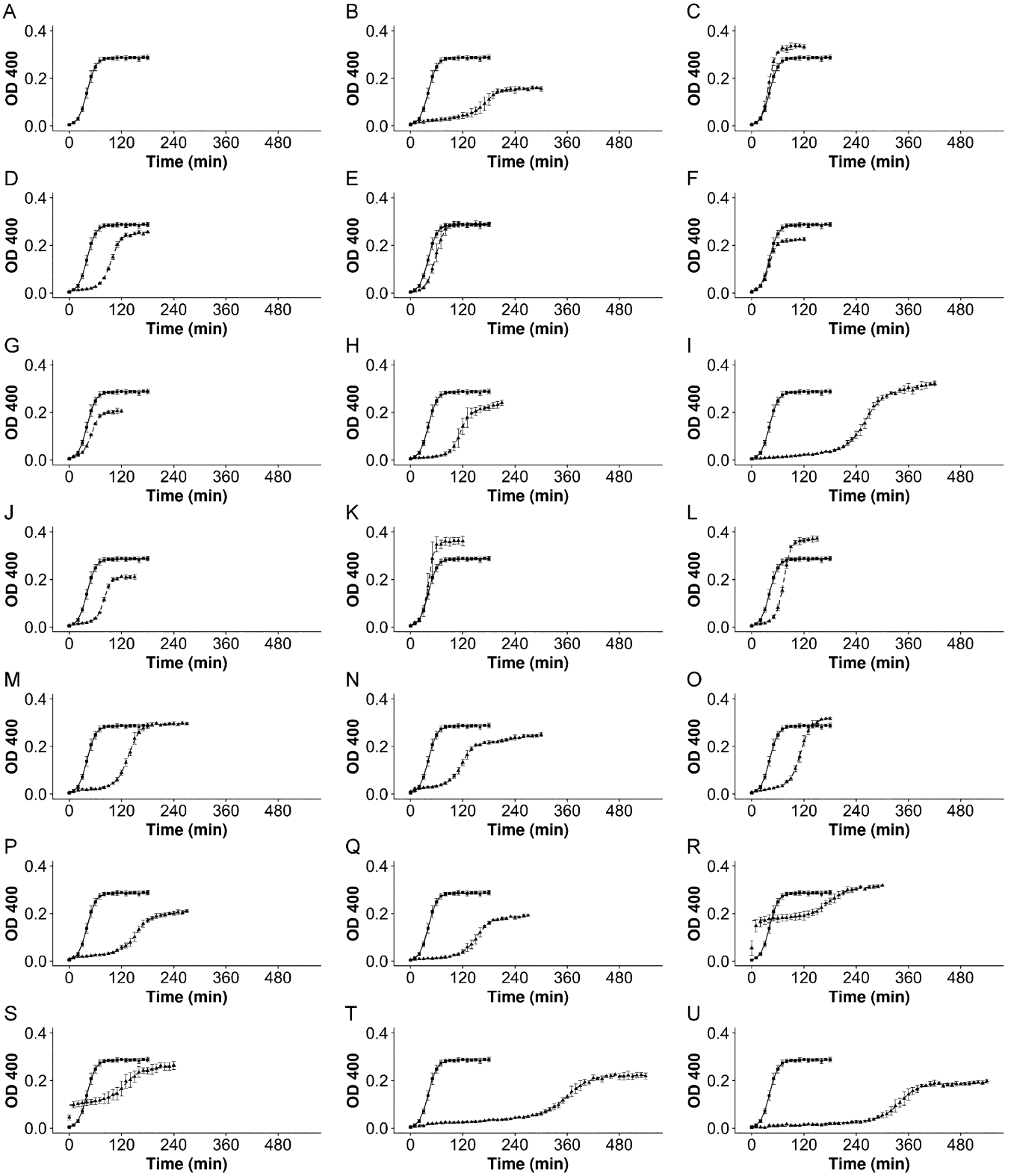

Fig. S3. Fibrillization kinetics assays of HET-s(218–289) mutants. (*A*) WT, (*B*) Δ251–253, (*C*) PA, (*D*) PB, (*E*) PAB, (*F*) SA-, (*G*) SB-, (*H*) SC-, (*I*) SABC-, (*J*) SB+, (*K*) SA+, (*L*) SC+, (*M*) SABC+, (*N*) NA, (*O*) NB, (*P*) NC, (*Q*) ND, (*R*) NAB, (*S*) NAD, (*T*) NBC, and (*U*) NCD. Points represent averaged data, error bars represent standard deviation, and lines indicate fitted curves. WT is shown as ■ and solid lines; mutants are shown as ▲ and dotted lines.

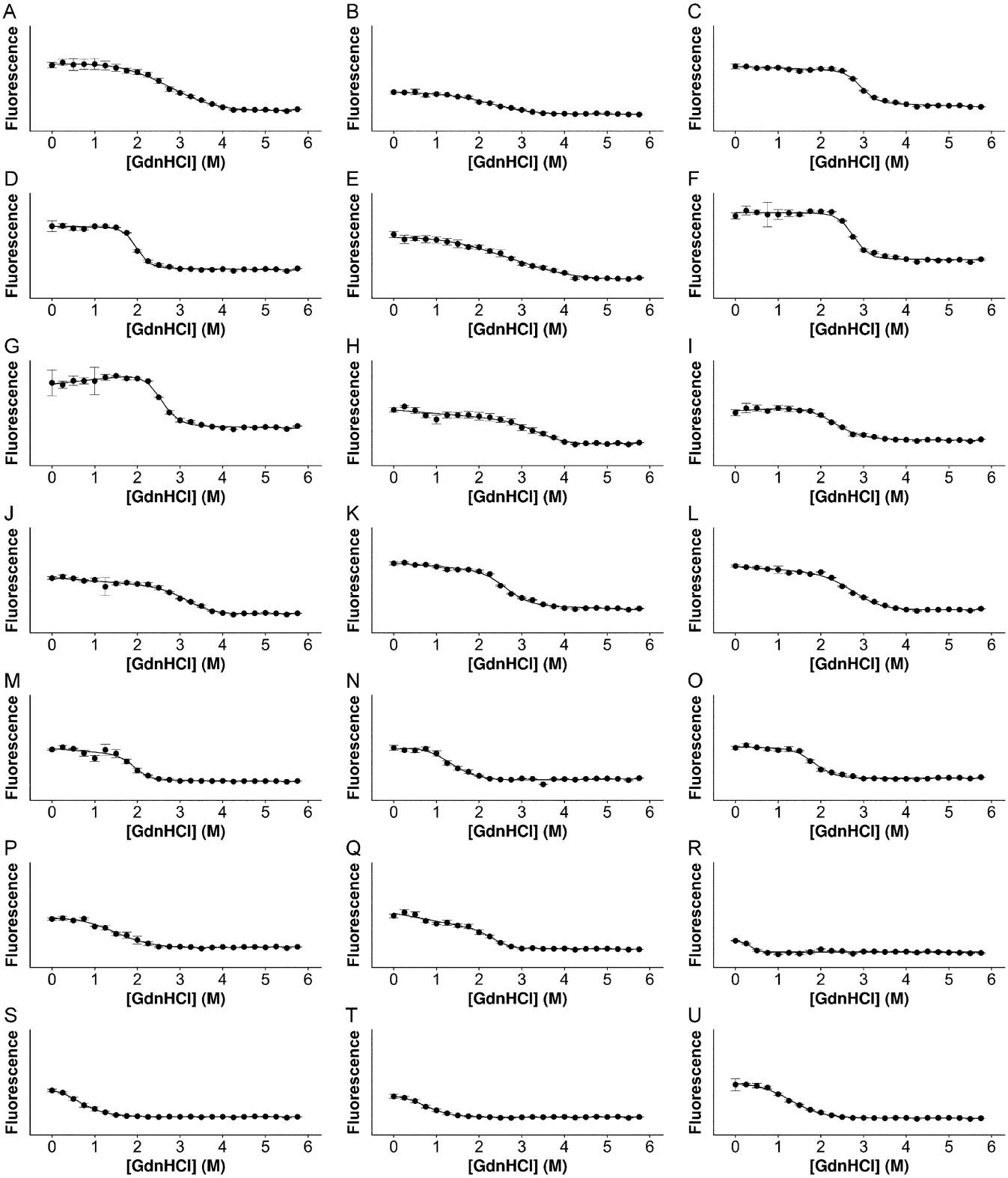

Fig. S4. Guanidine denaturation assays of HET-s(218–289) mutants. (*A*) WT, (*B*) Δ251–253, (*C*) PA, (*D*) PB, (*E*) PAB, (*F*) SA−, (*G*) SB−, (*H*) SC−, (*I*) SABC−, (*J*) SB+, (*K*) SA+, (*L*) SC+, (*M*) SABC+, (*N*) NA, (*O*) NB, (*P*) NC, (*Q*) ND, (*R*) NAB, (*S*) NAD, (*T*) NBC, and (*U*) NCD. ● represents averaged data points, error bars represent SD, and lines represent fitted curves.

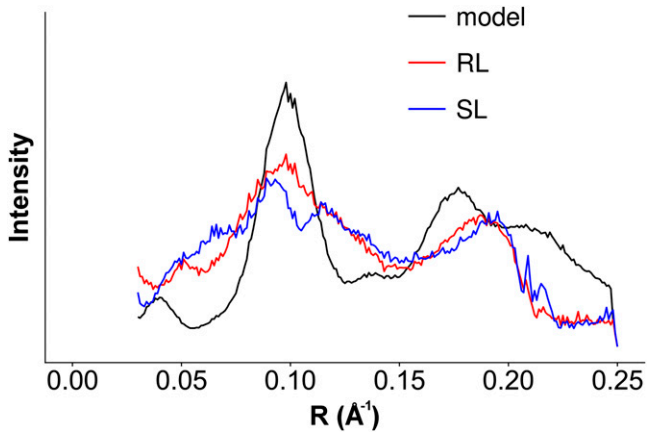

Fig. S5. Equatorial plots calculated from the stacked-sheet model, experimentally observed from RL and experimentally observed from SL.

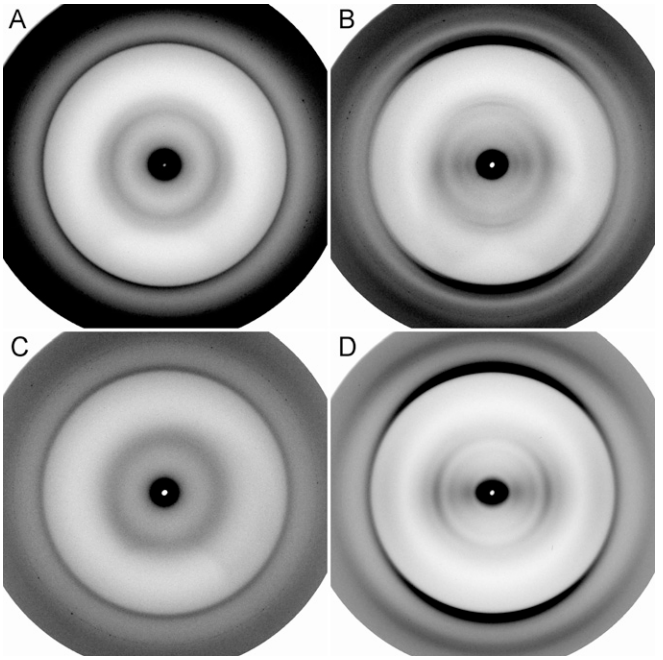

Fig. S6. X-ray fiber diffraction from HET-s(218–289) seeded with WT fibrils. (*A*) RL, (*B*), SL, (*C*) SN-, and (*D*) SN+.

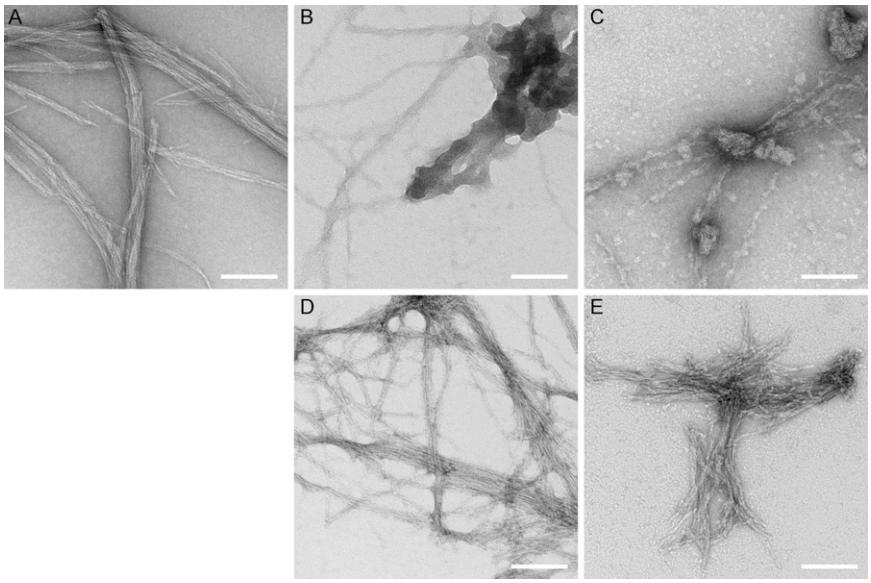

Fig. S7. Negative-stain EM of HET-s(218–289) WT and double asparagine-ladder mutants. (*A*) Mature WT, (*B*) NAB at 30 min, (*C*) NAD at 30 min, (*D*) NAB at 4 h, and (*E*) NAD at 4 h. (Scale bars, 100 nm.)

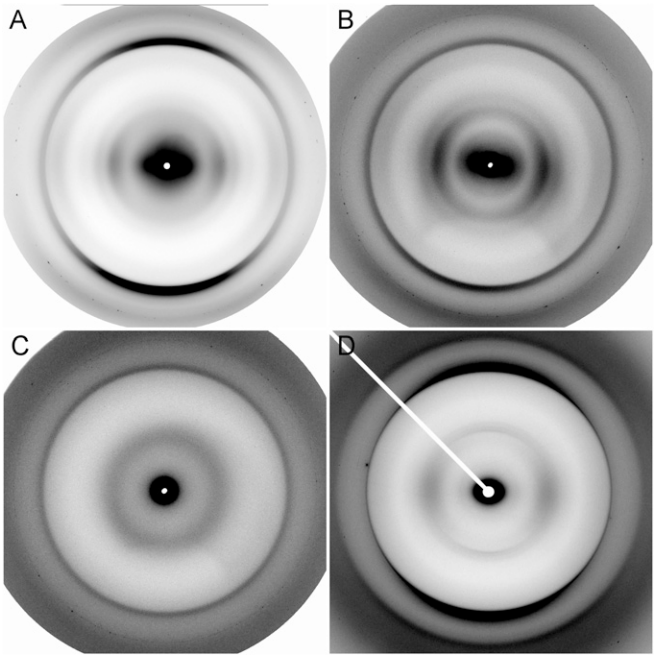

Fig. S8. X-ray fiber diffraction from double asparagine-ladder mutants at pH 4.0. (*A*) NAB, (*B*) NAD, (*C*) NBC, and (*D*) NCD.

Table S1. D spacings for disoriented fiber diffraction specimens

Mutant	Meridional	Equatorial	Rings
WT	9.47, 8.70, 4.83, 4.70	16.3, 10.6, 5.66	—
SABC+	9.61, 8.68, 4.82, 4.70	16.5, 11.0, 5.67	—
NAD	9.54, 8.52, 4.84, 4.72	16.3, 10.7, 5.71	—
NBC	9.42, 8.64, 4.70	16.1, 10.7, 5.59	—
SN−	—	—	4.45, 9.91
SN+	—	—	4.48, 9.84

Diffraction patterns with no orientation and no discernible axes are tabulated as rings.